



# Optimization of VQE-UCC Algorithm Based on Spin State Symmetry

Qing Guo<sup>1,2</sup> and Ping-Xing Chen<sup>1,2\*</sup>

<sup>1</sup>Department of Physics, College of Liberal Arts and Sciences, National University of Defense Technology, Changsha, China,

<sup>2</sup>Interdisciplinary Center for Quantum Information, National University of Defense Technology, Changsha, China

The accurate calculation of molecular energy spectra, a very complicated work, is of importance in many applied fields. Relying on the VQE-UCC algorithm, it is very possible to calculate the molecular energy spectrum on a noisy intermediate scale quantum computer. However, due to the limitation of the number of qubits and coherent time in quantum computers, the complexity of VQE-UCC algorithm still needs to be reduced in the simulation of macromolecules. We develop a new VQE-UCC method to calculate the ground state of the molecule according to the symmetry of the system, the complexity of which is reduced. Using this method we get the ground and excite state of four kinds of molecules. The method and the results are of great significance for the promotion of quantum chemical simulations.

## OPEN ACCESS

### Edited by:

Alexandre M Souza,  
Centro Brasileiro de Pesquisas  
Físicas, Brazil

### Reviewed by:

Che-Ming Li,  
National Cheng Kung University,  
Taiwan  
Yongjian Han,  
University of Science and Technology  
of China, China

### \*Correspondence:

Ping-Xing Chen  
pxchen@nudt.edu.cn

### Specialty section:

This article was submitted to  
Quantum Engineering and  
Technology,  
a section of the journal  
Frontiers in Physics

Received: 02 July 2021

Accepted: 10 September 2021

Published: 30 September 2021

### Citation:

Guo Q and  
Chen P-X (2021) Optimization of VQE-  
UCC Algorithm Based on Spin  
State Symmetry.  
Front. Phys. 9:735321.  
doi: 10.3389/fphy.2021.735321

**Keywords:** quantum computation, variational quantum eigensolver, unitary coupled cluster, quantum chemical, quantum simulation

## INTRODUCTION

In this year, quantum computing has been widely concerned as a new paradigm of computing. Compared with classical computing, the computing power of quantum computing increases exponentially with the increase of the number of qubits. One of the most likely applications of quantum computers is to simulate quantum mechanical systems [1], which is made possible by the emergence of some algorithms [2, 3] and later quantum processors [4, 5]. Molecule is one of the common quantum systems in nature. Calculating the energy spectra of a molecular system is one of the main goals of quantum chemistry, so the algorithm of simulating quantum chemistry by the noisy intermediate scale quantum computer (NISQ) has been of interest. However, due to the limitation of the number of qubits and coherent time of NISQ, there is still difficulties for us to simulate for macromolecules.

There are many methods having been used to reduce the complexity of quantum chemistry simulation, such as hybrid quantum classical algorithm (HQC) [6]. One of the most important algorithm is the variational quantum eigensolver (VQE) algorithm [7]. The VQE algorithm is based on the Ritz variational principle. The preparation of the ansatz and the measurement of the expected value of the Hamiltonian are carried out on the quantum computer. Then the classical computer optimizes the iterative parameters of the next ansatz according to the principle of minimizing the expected value of the Hamiltonian. The VQE algorithm can be used to find the molecular ground state energy. Compared with pure quantum algorithm, the VQE algorithm uses shorter quantum circuits and has stronger fault tolerance, but needs more measurements and the assistance of classical processes.

The two main steps of implementing VQE algorithm on NISQ are the selection of initial states and to effectively prepare the ansatz. The initial state is generally prepared into Hatree-Fock state. Because the Hatree-Fock method does not take into account the dynamic interaction between

electrons, it cannot obtain accurate electron energy. To prepare the ansatz, one mainly chooses the unitary coupled cluster method (UCC) [8, 9], coming from the classical single reference coupled cluster method (SRCC) [10, 11], which is more suitable for quantum computers. It divides the electron orbitals into two parts, the occupied orbitals and the unoccupied orbitals. Beginning with initial state (the Hartree-Fock state), a series of single excitation, double excitation and higher excitation operators which excite the electrons from the occupied orbitals to the unoccupied orbitals are applied to the initial state. After many rounds of operators, one may get the real ground state of the Hamiltonian. The details will be described in the second section. Some works have shown its accuracy. However, due to the limitation of the number of qubits and coherent time in quantum computers [12], it is still a great challenge for macromolecules to implement VQE-UCC algorithm on quantum computers.

In this paper, we propose a simpler UCC variant method, the singlet and pair UCC (SPUCC), based on the spin symmetry of molecules. In this method, the single excitation is classified and the double excitation only retains the pair excitation. The method can reduce the computational complexity while keeping the computational accuracy. Based on this method, we calculate the grounds of molecules with different structures and properties, and get good results as expected.

## METHOD OF SINGLET AND PAIR UNITARY COUPLED CLUSTER

Now we will introduce all the steps of realizing quantum chemical simulation on a quantum computer.

### The Second-Quantization of Molecular Hamiltonian

Using the Born-Oppenheimer approximation (B-O approximation), the Hamiltonian of the molecule can be written as:

$$\hat{H} = -\sum_i \frac{\nabla_i^2}{2} - \sum_{i,\alpha} \frac{Z_\alpha}{|r_i - R_\alpha|} + \sum_{ij} \frac{1}{2|r_i - r_j|} + E_N \quad (1.1)$$

Where  $R_\alpha$  represents the coordinates of the  $\alpha$ -th nucleus and  $Z_\alpha$  its charge number. Similarly,  $r_i$  represents the coordinates of the  $i$ -th electron. The first term of the Hamiltonian describes the kinetic energy of electrons, the second term describes the Coulomb interaction between nuclei and electrons, and the third term describes the Coulomb interaction between different electrons.  $E_N$  represents the kinetic energy of the nucleus and the Coulomb potential between different nuclei, which is constant when the nuclear coordinates are fixed.

In the second quantization, the wave function of the fermion is written as the fermion creation operator acting on the vacuum state. The creation operator and the annihilation operator can be identified as,

$$\{a_p^\dagger, a_q^\dagger\} = 0 \quad (1.2a)$$

$$\{a_p, a_q\} = 0 \quad (1.2b)$$

$$\{a_p, a_q^\dagger\} = \delta_{p,q} \quad (1.2c)$$

After the second quantization is introduced, the Hamiltonian in Eq. 1.1 can be written as,

$$\hat{H} = \sum_{p,q} h_{pq} a_p^\dagger a_q + \frac{1}{2} \sum_{p,q,r,s} h_{pqrs} a_p^\dagger a_q^\dagger a_r a_s + E_N \quad (1.3)$$

where,

$$h_{pq} = \int d\mathbf{x} \varphi_p^*(\mathbf{x}) \left( -\frac{\nabla_i^2}{2} - \sum_{\alpha} \frac{Z_\alpha}{|r_i - R_\alpha|} \right) \varphi_q(\mathbf{x}) \quad (1.4a)$$

$$h_{pqrs} = \int d\mathbf{x}_1 d\mathbf{x}_2 \frac{\varphi_p^*(\mathbf{x}_1) \varphi_q^*(\mathbf{x}_2) \varphi_r(\mathbf{x}_2) \varphi_s(\mathbf{x}_1)}{|\mathbf{x}_1 - \mathbf{x}_2|} \quad (1.4b)$$

The wave function  $\varphi_q(\mathbf{x})$ s are the basis functions we have chosen. The basis functions are usually related to the atomic orbitals and the figure base function [13, 14]. Their choice affect the accuracy of the calculation. Because of the cost, we chose the minimum basis set STO-3G.

### Encoding to Quantum State

In order to simulate quantum chemistry on a quantum computer, we use Jordan-Wigner (J-W) transformation [15] to map the contents of the above-mentioned second quantization to the quantum computer. In the J-W transformation, the creation and annihilation operator are designed as,

$$a_p^\dagger = \left( \prod_{i < p} \sigma_i^z \right) \sigma_p^+ \quad (2.1a)$$

$$a_p = \left( \prod_{i < p} \sigma_i^z \right) \sigma_p^- \quad (2.1b)$$

Where  $\sigma^+$  and  $\sigma^-$  are Pauli rise and fall operators,

$$\sigma^+ = \begin{pmatrix} 0 & 1 \\ 0 & 0 \end{pmatrix} \quad (2.2a)$$

$$\sigma^- = \begin{pmatrix} 0 & 0 \\ 1 & 0 \end{pmatrix} \quad (2.2b)$$

In this way, the Hamiltonian in Eq. 1.3 is transformed into the continuous product of a series of Pauli operators,

$$\hat{H} = C^0 I + \sum_p C_p^1 \sigma_p + \sum_{p,p'} C_{pp'}^2 \sigma_p \sigma_{p'} + \sum_{p,p',p''} C_{p,p',p''}^3 \sigma_p \sigma_{p'} \sigma_{p''} + \dots \quad (2.3)$$

The above-mentioned  $C^0$ ,  $C_p^1$  are constant, and  $\sigma_p$  represents the Pauli operator  $\sigma^x$ ,  $\sigma^y$  or  $\sigma^z$  of the  $a$ -th qubit.

### The Variational Quantum Eigensolver

The VQE algorithm uses the quantum computer to prepare quantum states and to get the expected value of Hamiltonian, which are difficult for the classical computer. The tedious process

of parameter optimization is handed over to the classical computer. It is based on Rayleigh-Ritz variational principle,

$$E_0 \leq \frac{\langle \psi(\vec{\theta}) | \hat{H} | \psi(\vec{\theta}) \rangle}{\langle \psi(\vec{\theta}) | \psi(\vec{\theta}) \rangle} \quad (3.1)$$

It shows that for a parameterized quantum state  $|\psi(\vec{\theta})\rangle$  we take randomly, the expected value of the Hamiltonian will always be greater than or equal to its minimum eigenvalue. The inequality can get the equal sign only if  $|\psi(\vec{\theta})\rangle$  is the real ground state  $|\psi_0\rangle$ .

To get the ground state, we usually start from the Hartree-Fock state. Selecting parameterize  $\vec{\theta}_1 = (\theta_1^1, \theta_1^2, \dots, \theta_1^k)$ , and then using  $|\psi(\vec{\theta})\rangle = U(\vec{\theta})|\varphi_0\rangle$  to realize the prepared state,

$$|\psi(\vec{\theta}_1)\rangle = U(\vec{\theta}_1)|\varphi_0\rangle \quad (3.2)$$

$$E(\vec{\theta}_1) = \frac{\langle \psi(\vec{\theta}_1) | \hat{H} | \psi(\vec{\theta}_1) \rangle}{\langle \psi(\vec{\theta}_1) | \psi(\vec{\theta}_1) \rangle} \quad (3.3)$$

We feedback the measured  $E(\vec{\theta}_1)$  to the classical computer and get the  $\vec{\theta}_2$  according to the optimization algorithm, taking  $|\psi(\vec{\theta}_1)\rangle$  as the initial state for next step,

$$|\psi(\vec{\theta}_2)\rangle = U(\vec{\theta}_2)|\psi(\vec{\theta}_1)\rangle \quad (3.4)$$

Then repeat the above steps to get  $E(\vec{\theta}_n)$  until the energy converges and then,

$$|\psi(\vec{\theta}_n)\rangle = U(\vec{\theta}_n)|\psi(\vec{\theta}_{n-1})\rangle \approx |\psi_0\rangle \quad (3.5)$$

$$E(\vec{\theta}_n) \approx E_0 \quad (3.6)$$

## Unitary Couple Cluster

The UCC is an improved version of the classical CC method, and the parameterized system wave function is given by the CC method,

$$|\psi(\vec{\theta})\rangle = e^{T(\vec{\theta})}|\varphi_0\rangle \quad (4.1)$$

The  $|\varphi_0\rangle$  is usually the Hartree-Fock state, and  $\vec{\theta}$  is the CC amplitude vector,  $T(\vec{\theta})$  is the excitation operator, defined as

$$T(\vec{\theta}) = \sum_{k=1}^n T_k(\vec{\theta}) \quad (4.2)$$

$$T_1(\vec{\theta}) = \sum_{i,j} \theta_{ij}^1 a_i^\dagger a_j \quad (4.3)$$

$$T_2(\vec{\theta}) = \sum_{i,j,k,l} \theta_{ijkl}^2 a_i^\dagger a_j^\dagger a_k a_l \quad (4.4)$$

...

For the trade-off between efficiency and accuracy, we usually intercept double excitations. Because the Hamiltonian mainly involves the interaction between monomer and two electrons, and then it can be proved that higher-order excitations can be composed of a combination of single and double excitations, resulting in coupled cluster single and double excitation methods (CCSD) [16].

By UCC method, the trial ansatz state is

$$|\psi(\vec{\theta})\rangle = e^{T(\vec{\theta})-T^\dagger(\vec{\theta})}|\varphi_0\rangle \quad (4.5)$$

Since  $T(\vec{\theta}) - T^\dagger(\vec{\theta})$  is an anti-Hermitian operator, so  $e^{T(\vec{\theta})-T^\dagger(\vec{\theta})}$  means a unitary evolution.

## Symmetry Optimization

However, for many molecules, some of its own characteristics are also important factors that can reduce the cost of quantum chemical simulation, such as the number of electrons and wave function symmetry of molecules. For a definite molecule, then the selected basis function can be reduced to a smaller subspace. So the excitation operator that keeps the spin symmetry plays an important role. Based on this idea, we divide the single excitation operator into two categories:

$$T_1^0 = \sum_{m,n} (a_{m\uparrow}^\dagger a_{n\uparrow} + a_{m\downarrow}^\dagger a_{n\downarrow}) \quad (5.1)$$

$$T_1^1 = \sum_{m,n} (a_{m\uparrow}^\dagger a_{n\uparrow} - a_{m\downarrow}^\dagger a_{n\downarrow}) \quad (5.2)$$

This classification is similar to the singlet unitary coupled cluster (UCCD0) method [17, 18],

$$T_2^0 = \sum_{i,j,k,l} (a_{i\uparrow}^\dagger a_{j\downarrow}^\dagger + a_{j\uparrow}^\dagger a_{i\downarrow}^\dagger) (a_{k\downarrow} a_{l\uparrow} + a_{l\downarrow} a_{k\uparrow}) \quad (5.3)$$

$$T_2^1 = \sum_{i,j,k,l} \left[ (a_{i\uparrow}^\dagger a_{j\downarrow}^\dagger - a_{j\uparrow}^\dagger a_{i\downarrow}^\dagger) (a_{k\downarrow} a_{l\uparrow} - a_{l\downarrow} a_{k\uparrow}) + a_{i\uparrow}^\dagger a_{j\uparrow}^\dagger a_{k\uparrow} a_{l\uparrow} + a_{i\downarrow}^\dagger a_{j\downarrow}^\dagger a_{k\downarrow} a_{l\downarrow} T_2^0 \right] \quad (5.4)$$

Where the triplet-paired operator  $T_2^1$  give rise a electrons triplet and  $T_2^0$  give rise a electrons singlet.

It is mainly based on the fact that  $T_1^0$  and  $T_2^0$  acting on any wave function will not change the symmetry of the states while  $T_1^1$  and  $T_2^1$  may change the state's symmetry. For most molecules, we think that the HF state and the real ground state should have the same symmetry, so we reduce  $T(\vec{\theta})$  to:

$$T(\vec{\theta}) = T_1^0 + T_2^0 \quad (5.5)$$

This method only retains the excited channel which keep the symmetry begin and after excitation. The number of excitation operator terms involved is  $O(n^4)$ .

However,

$$\begin{aligned}
 & a_{i\uparrow}a_{i\downarrow}(a_{i\uparrow}^\dagger a_{j\uparrow} + a_{i\downarrow}^\dagger a_{j\downarrow}) \\
 &= (a_{i\uparrow}a_{i\downarrow}a_{i\uparrow}^\dagger a_{j\uparrow} + a_{i\uparrow}a_{i\downarrow}a_{i\downarrow}^\dagger a_{j\downarrow}) \\
 &= (a_{i\uparrow}a_{j\downarrow} - a_{i\downarrow}a_{j\uparrow}) \\
 &= (a_{i\uparrow}a_{j\downarrow} + a_{j\uparrow}a_{i\downarrow})
 \end{aligned} \tag{5.6}$$

Similarly,

$$(a_{m\uparrow}^\dagger a_{n\uparrow} + a_{m\downarrow}^\dagger a_{n\downarrow})a_{n\downarrow}^\dagger a_{n\uparrow}^\dagger = (a_{m\uparrow}^\dagger a_{n\downarrow}^\dagger + a_{n\uparrow}^\dagger a_{m\downarrow}^\dagger) \tag{5.7}$$

Combining Eqs. 5.6, 5.7 we have

$$\begin{aligned}
 & (a_{m\uparrow}^\dagger a_{n\uparrow} + a_{m\downarrow}^\dagger a_{n\downarrow})a_{n\downarrow}^\dagger a_{n\uparrow}^\dagger a_{i\uparrow}a_{i\downarrow}(a_{i\uparrow}^\dagger a_{j\uparrow} + a_{i\downarrow}^\dagger a_{j\downarrow}) \\
 &= (a_{m\uparrow}^\dagger a_{n\downarrow}^\dagger + a_{n\uparrow}^\dagger a_{m\downarrow}^\dagger)(a_{i\uparrow}a_{j\downarrow} + a_{j\uparrow}a_{i\downarrow})
 \end{aligned} \tag{5.8}$$

So we can replace the operator  $T_2^0$  involving four index with a combination of two  $T_1^0$  and a pair of excitation operators. The unitary evolution is

$$U(\vec{\theta}) = e^{T_1^0(\vec{\theta})-h.c.} e^{T_{pair}(\vec{\theta})-h.c.} e^{T_1^0(\vec{\theta})-h.c.} \tag{5.9}$$

$$T_{pair}(\vec{\theta}) = \sum_{m,n} a_{m\downarrow}^\dagger a_{m\uparrow}^\dagger a_{n\uparrow} a_{n\downarrow} \tag{5.10}$$

The number of excitation operators involved in this method is  $3n^2$ . We can get

$$\begin{aligned}
 U(\vec{\theta}) &= (1 + T_1^0(\vec{\theta}) - h.c. + \dots)(1 + T_{puccd}(\vec{\theta}) - h.c. + \dots) \\
 (1 + T_1^0(\vec{\theta}) - h.c. + \dots) &= (1 + \dots + T_1^0(\vec{\theta})T_{puccd}(\vec{\theta})) \\
 T_1^0(\vec{\theta}) + \dots &= (1 + \dots + (a_{m\uparrow}^\dagger a_{n\uparrow} + a_{m\downarrow}^\dagger a_{n\downarrow})a_{n\downarrow}^\dagger a_{n\uparrow}^\dagger a_{i\uparrow}a_{i\downarrow} \\
 & (a_{i\uparrow}^\dagger a_{j\uparrow} + a_{i\downarrow}^\dagger a_{j\downarrow}))
 \end{aligned} \tag{5.11}$$

by Taylor expansion. While in  $T_2^0$ :

$$\begin{aligned}
 & U(\vec{\theta}) \\
 &= (1 + T_2^0(\vec{\theta}) - h.c. + \dots) \\
 &= (1 + (a_{m\uparrow}^\dagger a_{n\downarrow}^\dagger + a_{n\uparrow}^\dagger a_{m\downarrow}^\dagger)(a_{i\uparrow}a_{j\downarrow} + a_{j\uparrow}a_{i\downarrow}) + \dots)
 \end{aligned} \tag{5.12}$$

### Complexity

Let us consider a molecule with  $2M$  orbitals and  $2m$  electrons. We need  $2M$  qubits to code quantum state. The HF state  $|\varphi_0\rangle$  is  $\prod_{k=1}^{2m} a_k^\dagger|0\rangle$ .  $2m$  electrons occupy first  $2m$  orbits, then one of electron is excited from the  $i$ th orbit to  $j$ th orbit in a single excitation operation. Two electrons are excited from the  $i$ th and  $j$ th orbits to the  $k$ th and  $l$ th orbits respectively in the double excitation.

For a single excitation,

TABLE 1 | Time cost.

Method	model time/s	H <sub>4</sub> (4,8)	H <sub>2</sub> O(6,10)	N <sub>2</sub> (6,10)
UCCSD		277.8	1872.3	1826.1
UCCD0		1119.5	2169.4	690.4
SPUCC		209.6	202.1	141.6

$$\begin{aligned}
 U_i^j(\theta) &= \exp[\theta(a_i^\dagger a_i - a_j^\dagger a_j)] \\
 &= \exp\left[-i\frac{\theta}{2}(X_i Y_j - Y_i X_j) \prod_{i+1}^{j-1} Z_r\right] \\
 &= \exp\left(-i\frac{\theta}{2}X_i Y_j \prod_{i+1}^{j-1} Z_r\right) * \exp\left(i\frac{\theta}{2}Y_i X_j \prod_{i+1}^{j-1} Z_r\right)
 \end{aligned} \tag{6.1}$$

According to the decomposition of the quantum circuit [19, 20], we need 10 single qubit gates and  $4(j-i)$  CNOT gates to implement the above single excitation quantum circuit.

For a double excitation, the unitary evolution operator can be expressed by Paul operators as follow,

$$\begin{aligned}
 U_{ij}^{kl}(\theta) &= \exp[\theta(a_k^\dagger a_i^\dagger a_j a_l - a_i^\dagger a_j^\dagger a_k a_l)] \\
 &= \exp\left[-i\frac{\theta}{8}\left(X_i Y_j X_i X_i + Y_i X_j X_i X_i + Y_i Y_i Y_i X_j + Y_i Y_i X_j Y_i - \right.\right. \\
 & \left.\left. X_i X_i Y_j X_i - X_j X_i X_i Y_j - Y_i X_j Y_i Y_i - X_j Y_i Y_i Y_i\right) \prod_{i+1}^{j-1} Z_r \prod_{k+1}^{l-1} Z_r\right],
 \end{aligned} \tag{6.2}$$

where  $i, j$  are the index of occupied orbit and  $k, l$  are the index of unoccupied orbit.

Similarly, it needs 72 single qubit gates and  $16(j+l-i-k)$  CNOT gates to implement the above double excitation quantum circuit. From Eq. 6.1 and Eq. 6.2, We can get clearly that the gate cost of each single or double excitation through J-W transformation is  $O(M)$ . UCCSD needs  $x = C_{2m}^1 * C_{2M-2m}^1 \sim (M-m)m < M^2$  single excitations and  $y = C_{2m}^2 * C_{2M-2m}^2 \sim (M-m)^2 m^2 < M^4$  double excitations. So its gate complexity is  $O(M^5)$ . UCCD0 needs  $x = C_{2m}^1 * C_{2M-2m}^1 \sim (M-m)m < M^2$  single excitations and  $y = C_m^2 * C_{M-m}^2 \sim (M-m)^2 m^2 < M^4$  double excitations. So its gate complexity is also  $O(M^5)$ .

While in SPUCC, we use the spin symmetry, the single excitation is  $\sum_{0 \leq i < m} (a_{j\uparrow}^\dagger a_{i\uparrow} + a_{j\downarrow}^\dagger a_{i\downarrow} - h.c.)$  and the double

excitation is  $\sum_{0 \leq i < m} (a_{j\uparrow}^\dagger a_{i\uparrow} + a_{j\downarrow}^\dagger a_{i\downarrow} - h.c.)$ . The  $j\uparrow$  and  $j\downarrow$

are the  $2j$ th and  $(2j-1)$ -th orbit. So it only needs  $x = C_m^1 * C_{M-m}^1 \sim (M-m)m < M^2$  single excitations and  $y = C_m^1 * C_{M-m}^1 \sim (M-m)m < M^2$  double excitations. Its gate complexity is  $O(M^3)$ .

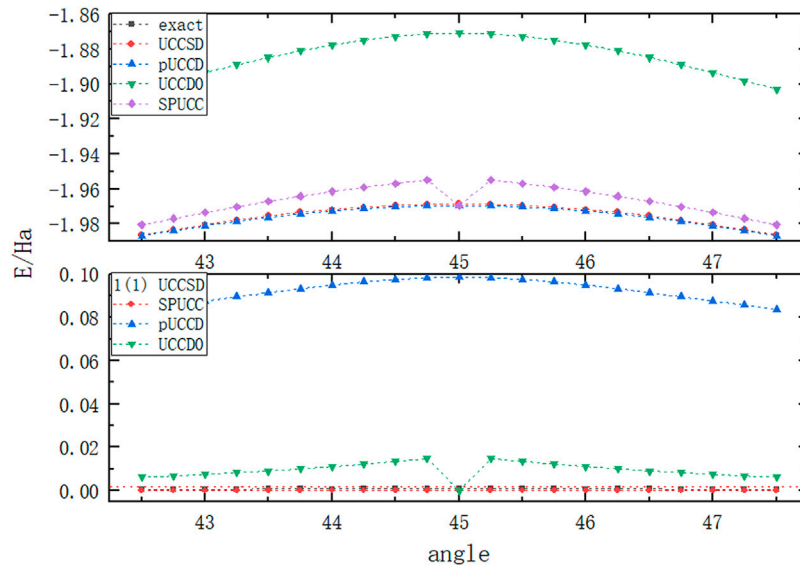


**FIGURE 1** | The picture above shows the variation of the energy of  $H_4$  molecule with the circumferential angle, and the figure below shows the difference of the energy of different methods and exact diagonalization from different angles. The red dotted line represents the chemical accuracy of  $1.6 \times 10^{-3} Ha$ .

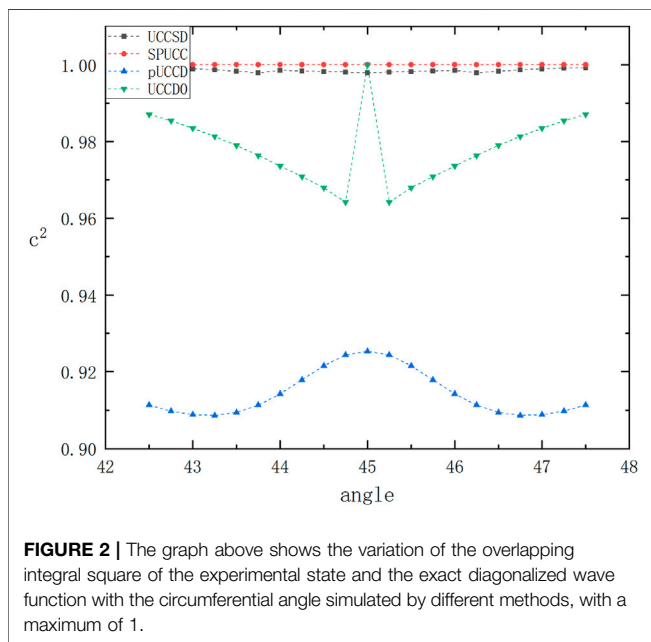


**FIGURE 2** | The graph above shows the variation of the overlapping integral square of the experimental state and the exact diagonalized wave function with the circumferential angle simulated by different methods, with a maximum of 1.

## RESULTS

We have studied four kinds of molecules  $H_2$ ,  $H_4$ ,  $H_2O$ , and  $N_2$ . We use Psi4 [21] and OpenFermion [22] to obtain molecular Hamiltonian and QuTip [23] to realize quantum state evolution. In order to discuss the accuracy of the method, we compare it with exact diagonalization and other UCC methods, i.e., UCCSD, pair unitary coupled cluster double (pUCCD) [24] and UCCD0.

At the same time, we compare the time cost of the three molecules simulated by different methods on the classical computer, which we think can be used as a qualitative

comparison of the complexity of the three methods. Because of the deviation of the pUCCD method, we do not evaluate its cost. For details, please see **Table 1**.

The data in the table is the time cost of different methods under this structure,  $H_4$  (1.738Å,  $45^\circ$ ),  $H_2O$  (1.2Å,  $104.5^\circ$ ),  $N_2$  (1.2Å). The tolerance of iterative energy is  $10^{-7}$ . For molecule  $H_2$ , it is too simple to show the superiority of SPUCC. It can be seen that SPUCC is better than other methods in all cases. It is affected by accuracy and molecular structure.

### Molecule $H_2$

Molecule  $H_2$  is the simplest molecule in chemistry and only involves two atoms and two electrons. So it has only two molecular orbitals (MOs) and four orthogonal states, which can be expressed as:

$$\begin{aligned} |\varphi_0\rangle &= a_{01}^+ a_{01}^+ |0\rangle \\ |\varphi_1\rangle &= (a_{11}^+ a_{01}^+ + a_{11}^+ a_{01}^+) |0\rangle \\ |\varphi_2\rangle &= (a_{11}^+ a_{01}^+ - a_{11}^+ a_{01}^+) |0\rangle \\ |\varphi_3\rangle &= a_{11}^+ a_{11}^+ |0\rangle \end{aligned}$$

Where,  $|\varphi_0\rangle$ ,  $|\varphi_1\rangle$  and  $|\varphi_3\rangle$  are singlet while  $|\varphi_2\rangle$  is triplet. By using the method in Ref. [25], we have calculated the excited state of molecule  $H_2$  ( $R = 0.7414\text{\AA}$ ) by using the initial VQE algorithm and obtained the following results.

$$\begin{aligned} |\psi_0\rangle &= 0.9936|\varphi_0\rangle - 0.1128|\varphi_3\rangle \\ |\psi_1\rangle &= |\varphi_1\rangle \\ |\psi_2\rangle &= |\varphi_2\rangle \\ |\psi_3\rangle &= 0.9936|\varphi_3\rangle - 0.1128|\varphi_0\rangle \end{aligned}$$

The results show that the ground state of molecule  $H_2$  is a singlet state. Correspondingly, the ground state obtained by VQE is also composed of a singlet state, which proves our idea to some extent.

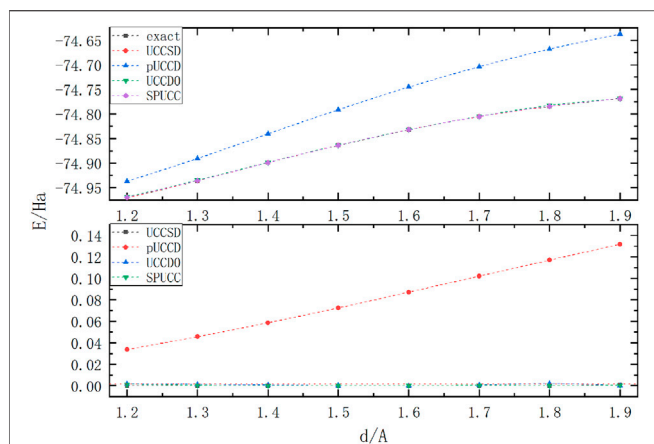


**FIGURE 3** | The graph above shows the energy of molecule  $H_2O$  ( $\alpha = 104.5^\circ$ ) varies with the bond length (6 electrons and 10 orbitals). The following figure shows the difference of the energy of each method and exact diagonalization with different bond lengths. The red dotted line represents the chemical precision of  $1.6 \times 10^{-3} Ha$ .

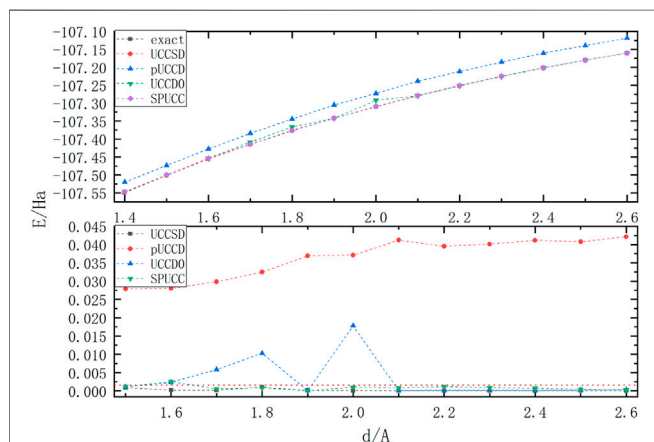


**FIGURE 4** | A graph in which the energy of a molecule  $N_2$  varies with bond length (6 electrons and 10 orbitals). The above picture shows the curve of the energy of each method in the bond dissociation region with the bond length, and the diagram below shows the relationship between the difference between each method and the diagonalization energy and the bond length. The red dotted line represents the chemical precision of  $1.6 \times 10^{-3} Ha$ .

## Molecule $H_4$

Molecule  $H_4$  is an unstable configuration. But because of its symmetry, it is often used as a criterion for evaluating different calculation methods [26].

The molecule  $H_4$  configuration calculated by us is an inscribed rectangle with a diameter of 1.738Å. By changing the circumferential angle  $\alpha$  of three atoms  $H$  from  $42.5^\circ$  to  $47.5^\circ$ , its symmetry slowly transitions from  $C_{2v}$  to  $C_{4v}$  and back to  $C_{2v}$ . We give the potential energy curve of molecule  $H_4$  calculated by exact diagonalization, UCCSD, pUCCD, UCCD0 and SPUCC in **Figure 1**.

It can be seen from **Figure 1** that there is a large energy deviation between pUCCD and UCCD0, while SPUCC shows the same accuracy as UCCSD. At the same time, UCCD0 shows the

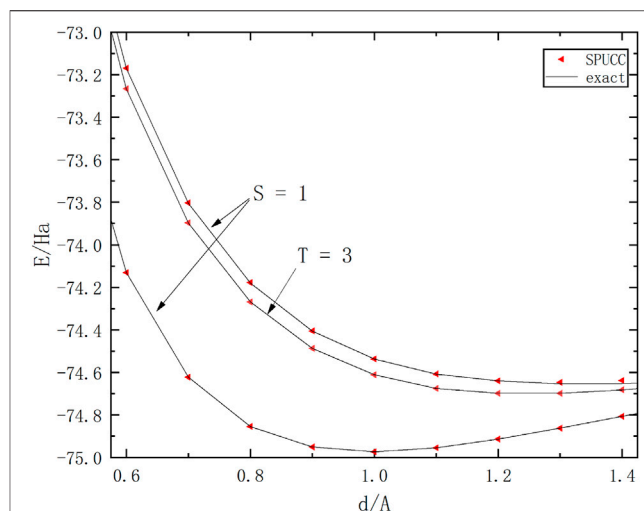


**FIGURE 5** | A graph in which the energy of a molecule  $H_2O$  varies with bond length (6 electrons and 10 orbitals). The  $S = 1$  represents the singlet state, and the  $T = 3$  represents the triplet state. From the bottom up, they are the ground state, the first and second excited states of the molecule.

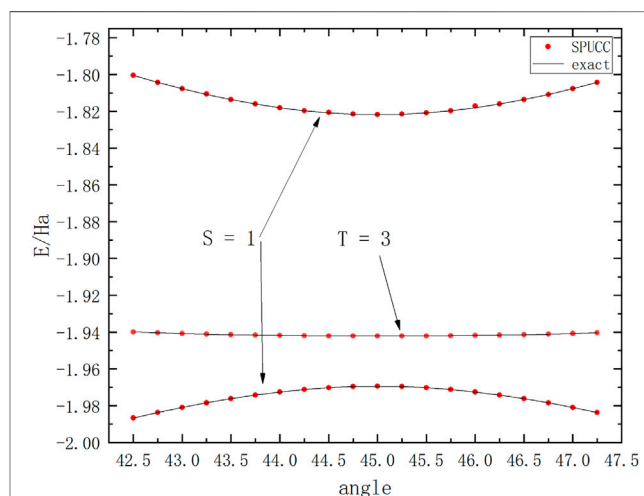


**FIGURE 6** | A graph in which the energy of a molecule  $H_4$  varies with bond length (6 electrons and 10 orbitals). The  $S = 1$  represents the singlet state, and the  $T = 3$  represents the triplet state. From the bottom up, they are the ground state, the first and second excited states of the molecule.

same superiority as SPUCC when the circumferential angle is  $42.5^\circ$ . **Figure 1** shows that the circumferential angle varies from  $42.5^\circ$  to  $47.5^\circ$ , and the offset calculated by SPUCC is within the range of chemical accuracy.

At the same time, we are also interested in studying the fidelity. The results have been shown in **Figure 2**. We can find that SPUCC shows better accuracy than the usual VQE-UCC method.

## Molecule $H_2O$

Molecule  $H_2O$  is the most common molecule in life. It acts as a solvent most of the time in chemistry and is very necessary to

understand its properties. It is unequal hybrid of  $sp^3$ , and the heterozygosity between the two atoms  $H$  and the vertex atom  $O$  is  $104.5^\circ$ .

**Figure 3** shows that all methods show high accuracy in  $d < 1.2A$ . When  $d \geq 1.2A$ , the pUCCD begins to shift, and other methods have good accuracy, and the maximum error shown by SPUCD on the graph is about  $1.15mHa$ .

## Molecule $N_2$

Because of the existence of three bonds with strong correlation, molecule  $N_2$  has become one of the strictest test cases of single reference electron structure. It has six active  $p$  electrons, which form several equivalent configurations at the bond dissociation limit.

In **Figure 4**, excepting for the offset of pUCCD, all the other methods have good accuracy. SPUCD shows better results than UCCD0 on the graph, and its maximum error is about  $2mHa$ .

## Excited State

On the basis of the previous work, we have studied the different molecular spin states. For example, the ground state and the second excited state (singlet state) and the first excited state (triplet state) of molecule  $H_2O$ . Because of the difference of symmetry, the SPUCD method will not fall into the triplet state from the test state of a singlet state. When using the method in Ref. [25], we do not operate when we calculate the singlet state, but when we calculate the triplet state, we use an excitation operator  $U = a_{m\uparrow}^\dagger a_{n\uparrow} - a_{m\downarrow}^\dagger a_{n\downarrow}$  to obtain a triplet state on the initial HF state, and then take the triplet state as the initial state. We have calculated the excited states of both molecule  $H_2O$  and molecule  $H_4$ . The results are shown in **Figures 5, 6** and is in line with expectations.

## CONCLUSION

The VQE-UCC method is a practical quantum algorithm for calculating molecular energy spectra. It can reproduce the exact electronic structure properties of many molecular systems within the range of chemical accuracy. The main reason for the success of this algorithm is its variational property. However, limited by the

current technology, the number of qubits and coherent time limit the scalability of the quantum chemistry simulation system. The complexity of UCCSD leads to the increase of quantum circuit depth, and our proposed UCC method variant SPUCD method reduces its complexity, correspondingly reduces the circuit depth of quantum simulation, and makes it more suitable for today's NISQ. We calculate the energy changes of a series of molecules along the bond length. Our simulations show correct qualitative dissociation curves, which are basically within the range of chemical accuracy on the whole dissociation curve. At the same time, we also calculate their excited states across spin symmetry, which provides some experience for us to calculate the excited states of molecules in the future. In a word, we prove that the potential of the SPUCD method proposed in this paper can be equal to that of the current variants, and it can also deal with the strong correlation system very well. The combination of this method with the recent VQE method is expected to open up a new possibility for the use of ground-depth circuits in NISQ to solve the electronic structure problems of macromolecular systems.

## DATA AVAILABILITY STATEMENT

The original contributions presented in the study are included in the article/Supplementary Material, further inquiries can be directed to the corresponding author.

## AUTHOR CONTRIBUTIONS

All authors listed have made a substantial, direct, and intellectual contribution to the work and approved it for publication.

## FUNDING

This work is supported by the National Basic Research Program of China under Grant No. 2016YFA0301903 and the National Natural Science Foundation of China under Grants No. 61632021, No. 11904402 and No. 12004430.

## REFERENCES

- Feynman RP. Quantum Mechanical Computers. *Found Phys* (1986) 16(6): 507–31. doi:10.1007/BF01886518
- Georgescu IM, Ashhab S, and Nori F. Quantum Simulation. *Rev Mod Phys* (2014) 86(1):153–85. doi:10.1103/RevModPhys.86.153
- Proceedings 35th Annual Symposium on Foundations of Computer Science. In: Paper presented at the Proceedings 35th Annual Symposium on Foundations of Computer Science; 20-22 Nov. 1994; Santa Fe, NM, USA. IEEE (1994). doi:10.1109/SFCS.1994.365747
- Kelly J. "Engineering Superconducting Qubit Arrays for Quantum Supremacy," in APS March Meeting 2018. American Physical Society (2018). <https://ui.adsabs.harvard.edu/abs/2018APS.MARA33001K>.
- Murali P, Linke N, Martonosi M, Abhari A, Nguyen N, and Huerta Alderete C. Full-Stack, Real-System Quantum Computer Studies: Architectural Comparisons and Design Insights. In: ISCA 19: The 46th Annual International Symposium on Computer Architecture; June 22 - 26, 2019; Phoenix AZ. Phoenix, AZ: Association for Computing Machinery (2019). p. 527–40. doi:10.1145/3307650.3322273
- McClellan JR, Romero J, Babbush R, and Aspuru-Guzik A. The Theory of Variational Hybrid Quantum-Classical Algorithms. *New J Phys* (2016) 18(2): 023023. doi:10.1088/1367-2630/18/2/023023
- Peruzzo A, McClellan J, Shadbolt P, Yung M-H, Zhou X-Q, and Love PJ. A Variational Eigenvalue Solver on a Photonic Quantum Processor. *Nat Commun* (2014) 5:4213. doi:10.1038/ncomms5213
- Hempel C, Maier C, Romero J, McClellan J, Monz T, and Shen H. Quantum Chemistry Calculations on a Trapped-Ion Quantum Simulator. *Phys Rev X* (2018) 8(3):031022. doi:10.1103/PhysRevX.8.031022
- Shen Y, Zhang X, Zhang S, Zhang J-N, Yung M-H, and Kim K. Quantum Implementation of the Unitary Coupled Cluster for Simulating Molecular Electronic Structure. *Phys Rev A* (2017) 95(2):020501. doi:10.1103/PhysRevA.95.020501
- Čížek J. On the Correlation Problem in Atomic and Molecular Systems. Calculation of Wavefunction Components in Ursell-Type Expansion Using Quantum-Field Theoretical Methods. *J Chem Phys* (1966) 45(11):4256–66. doi:10.1063/1.1727484

11. Bartlett RJ, and Musiał M. Coupled-cluster Theory in Quantum Chemistry. *Rev Mod Phys* (2007) 79:291–352. doi:10.1103/revmodphys.79.291
12. Preskill J. Quantum Computing in the NISQ Era and beyond. *Quantum* (2018) 2:79. doi:10.22331/q-2018-08-06-79
13. Jensen F. Atomic Orbital Basis Sets. *Wires Comput Mol Sci* (2013) 3:273–95. doi:10.1002/wcms.1123
14. Nagy B, and Jensen F. Basis Sets in Quantum Chemistry in: *Reviews in Computational Chemistry*. Chapter 3. Hoboken, NJ: Wiley Online Library (2017). p. 93–149.
15. Whitfield JD, Biamonte J, and Aspuru-Guzik A. Simulation of Electronic Structure Hamiltonians Using Quantum Computers. *Mol Phys* (2011) 109: 735–50. doi:10.1080/00268976.2011.552441
16. Wecker D, Hastings MB, and Troyer M. Progress towards Practical Quantum Variational Algorithms. *Phys Rev A: Mol Opt Phys* (2015) 92:042303. doi:10.1103/physreva.92.042303
17. Bulik IW, Henderson TM, and Scuseria GE. Can Single-Reference Coupled Cluster Theory Describe Static Correlation? *J Chem Theor Comput.* (2015) 11(7):3171–9. doi:10.1021/acs.jctc.5b00422
18. Gomez JA, Henderson TM, and Scuseria GE. Recoupling the Singlet- and Triplet-Pairing Channels in Single-Reference Coupled Cluster Theory. *J Chem Phys* (2016) 145(13):134103. doi:10.1063/1.4963870
19. Cao Y, Romero J, Olson JP, Degroote M, Johnson PD, and Kieferová M. Quantum Chemistry in the Age of Quantum Computing. *Chem Rev* (2019) 119(19):10856–915. doi:10.1021/acs.chemrev.8b00803
20. Romero J, Babbush R, McClean JR, Hempel C, Love PJ, and Aspuru-Guzik A. Strategies for Quantum Computing Molecular Energies Using the Unitary Coupled Cluster Ansatz. *Quan Sci. Technol.* (2018) 4(1):014008. doi:10.1088/2058-9565/aad3e4
21. Smith DGA, Burns LA, Simmonett AC, Parrish RM, Schieber MC, and Galvelis R. Psi4 1.4: Open-Source Software for High-Throughput Quantum Chemistry. *J Chem Phys* (2020) 152:184108. doi:10.1063/5.0006002
22. McClean JR, Rubin NC, Sung KJ, Kivlichan ID, Bonet-Monroig X, and Cao Y. OpenFermion: the Electronic Structure Package for Quantum Computers. *Quan Sci. Technol.* (2020) 5(3):034014. doi:10.1088/2058-9565/ab8ebc
23. Johansson JR, Nation PD, and Nori F. QuTiP 2: A Python Framework for the Dynamics of Open Quantum Systems. *Comp Phys Commun* (2013) 184(4): 1234–40. doi:10.1016/j.cpc.2012.11.019
24. Zhao L, and Neuscammann E. Amplitude Determinant Coupled Cluster with Pairwise Doubles. *J Chem Theor Comput.* (2016) 12:5841–50. doi:10.1021/acs.jctc.6b00812
25. Higgott O, Wang DS, and Brierley S. Variational Quantum Computation of Excited States. *Quantum* (2019) 3:156. doi:10.22331/q-2019-07-01-156
26. Genovese C, Meninno A, and Sorella S. Assessing the Accuracy of the Jastrow Antisymmetrized Geminal Power in the H4 Model System. *J Chem Phys* (2019) 150(8):084102. doi:10.1063/1.5081933

**Conflict of Interest:** The authors declare that the research was conducted in the absence of any commercial or financial relationships that could be construed as a potential conflict of interest.

**Publisher's Note:** All claims expressed in this article are solely those of the authors and do not necessarily represent those of their affiliated organizations, or those of the publisher, the editors and the reviewers. Any product that may be evaluated in this article, or claim that may be made by its manufacturer, is not guaranteed or endorsed by the publisher.

Copyright © 2021 Guo and Chen. This is an open-access article distributed under the terms of the Creative Commons Attribution License (CC BY). The use, distribution or reproduction in other forums is permitted, provided the original author(s) and the copyright owner(s) are credited and that the original publication in this journal is cited, in accordance with accepted academic practice. No use, distribution or reproduction is permitted which does not comply with these terms.